3) Always present a match to the signal generator such that the total power into the ring hybrid remains constant.

Referring to the variable power divider shown in Fig. 1(b),[1] and using the standard transmission line equations,[2] the voltages at terminals 1, 2, and 3 are related by

$$V_1 = jV_2\frac{Y_2}{Y_0} = jV_3\frac{Y_3}{Y_0} \tag{2}$$

where Y_2/Y_0 and Y_3/Y_0 are the normalized loads on arms 2 and 3, namely, matched external loads plus the susceptances of the short-circuited shunt arms at 2 and 3. Thus:

$$\begin{aligned}\frac{Y_2}{Y_0} &= 1 + j\tan\left(\frac{2\pi l}{\lambda} + \frac{\pi}{2}\right)\\ &= 1 - j\operatorname{ctn}\frac{2\pi l}{\lambda}\\ \frac{Y_3}{Y_0} &= 1 + j\tan\frac{2\pi l}{\lambda}.\end{aligned} \tag{3}$$

Combining (2) and (3), we obtain

$$\frac{V_2}{V_3} = \frac{Y_3}{Y_2} = \frac{1 + j\tan\dfrac{2\pi l}{\lambda}}{1 - j\operatorname{ctn}\dfrac{2\pi l}{\lambda}} = j\tan\frac{2\pi l}{\lambda}. \tag{4}$$

If power divider arms 2 and 3 are connected to terminals 4 and 1 of the ring hybrid, then V'/V is equal to $\tan 2\pi l/\lambda$ and (1) may be written as

$$\frac{V_{2T}}{V_{3T}} = e^{j(4\pi l/\lambda)}. \tag{5}$$

Thus, the relative phase between outputs 2 and 3 of the ring hybrid varies linearly with the variable length l of the power divider. Note that the phase change produced is twice the change in electrical length of l. To prove that the power input to the ring hybrid remains constant, we will calculate the input admittance at terminal 1 of the power divider and show that it is invariant with l. The total current at terminal 1 is the sum of the currents I_{12} and I_{13} flowing toward loads 2 and 3 respectively. Using the transmission line equations,[3] we can write

$$\begin{aligned}I_{12} &= jV_2Y_0\\ I_{13} &= jV_3Y_0.\end{aligned} \tag{6}$$

Adding (6) and substituting (2) and (3), we have

$$\begin{aligned}I_1 &= I_{12} + I_{13} = jY_0(V_2 + V_3)\\ &= Y_0V_1\left(\frac{Y_0}{Y_2} + \frac{Y_0}{Y_3}\right)\\ Y_1 = \frac{I_1}{V_1} &= Y_0\left\{\frac{1}{1 - j\operatorname{ctn}\dfrac{2\pi l}{\lambda}} + \frac{1}{1 + j\tan\dfrac{2\pi l}{\lambda}}\right\} = Y_0.\end{aligned}$$

Hence, the admittance at input terminal 1 of the power divider is independent of l and matched to the line.

Equivalent forms of the devices shown in Fig. 1 are realizable in waveguide, coax, stripline, and lumped circuits. The technique, therefore, is applicable over a wide range of frequencies. Not only is the number of separate components reduced relative to the conventional fixed power divider dual phase shifter approach previously mentioned, but the technique should also be substantially more compact from a mechanical point of view relative to ganged and oppositely driven dual phase shifters.

Experimental Results

A variable power divider was constructed of rigid coax and coupled to a stripline hybrid via equilength flexible cables at 2300 Mc. Although the ideal conditions assumed in the analysis were not fully realized, a phase deviation of less than $\pm 10°$ and an amplitude variation of less than 1 db from that predicted by (5) was observed over a range of 360°. In general, it is believed that the degree to which the measured performance will deviate from the ideal is largely determined by the power divider. It has been shown that the power divider voltage output ratio must vary according to the function $\tan 2\pi l/\lambda$. In a practical situation the instantaneous 180° phase change of the tangent function as l goes through $\lambda/4$ is only a gradual one. Somewhat compensating for this gradual change in phase is the fact that practically all of the signal emerges from only one arm of the power divider over this range of l. Work on the power divider should produce the most fruitful results in future development of this technique.

E. J. Wilkinson
F. LaRussa
Antenna and Microwave Lab.
Sylvania Electric Products, Inc.
Waltham, Mass.

A Beam Plasma Surface Wave Interaction*

This communication describes the interaction of an electron beam with a beam-generated hydrogen plasma. As a result of this interaction the dc energy of the electron beam is converted into microwave energy in the plasma.

The experimental system is shown in Fig. 1. Coupling helices with essentially zero-db gain are located on both sides of an interaction cavity. An immersed gun of perveance 10^{-6} is used, and beam voltages are of the order of 660 volts. An axial magnetic field in the range of 500–1000 gauss focuses the beam. The system is pumped out, and gas is introduced by heating a titanium hydride capsule; this increases the pressure to the vicinity of 10^{-2} mm Hg. Beam electron collisions then ionize many of these hydrogen atoms, creating an electron density of approximately 10^{11} electrons/cm^3. As a result of the beam collision process, the plasma exists only in the immediate vicinity of the beam, so that the model which is assumed is that of a plasma column partially filling a cylindrical waveguide, with the plasma radius much smaller than the waveguide radius. The cross-section model is shown in Fig. 2.

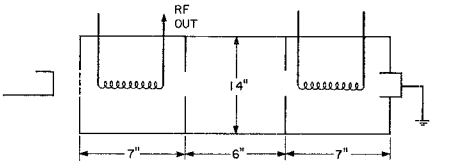

Fig. 1—Simplified experimental system.

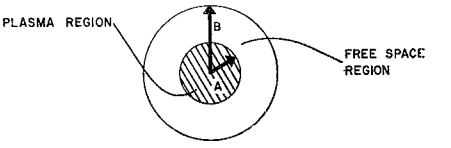

Fig. 2—Cross section of plasma column.

The results of the experiment are given by the following. With no signal applied to either helix, an RF signal higher than the cyclotron frequency is observed on the first helix as shown in Fig. 1. The signal, however, is not observed on the second helix. This signal is in the kilomegacycle region, and has a bandwidth of approximately 10 Mc. Its power was measured to be as high as 720 Mw, which, on the basis of 11-w input beam power, represents an efficiency of 6.5 per cent. Signals of a much lower power level were observed 80 Mc on each side of the center frequency; these sidebands were interpreted to be associated with ion plasma oscillations. By multiplying the ion plasma frequency by the square root of the mass ratio of electrons and ions, the electron plasma frequency can be computed to be 3200 Mc.

The plasma mode with which the beam interacts is identified as the angularly symmetric forward wave mode discussed by Gould and Trivelpiece[1] and Smullin and Chorney.[2] The ω-β curve of this mode for the case of $\omega_p > \omega_c$ is shown in Fig. 3. By intersecting the velocity line of the beam ($v/c = 0.05$) with the plasma ω-β curve for actual operating values of ω_c and ω_p, it is found that the intersection occurs at a frequency which is, in fact, the observed output frequency. (This process is actually per-

[1] G. L. Ragan, Ed., "Microwave Transmission Circuits," M.I.T. Rad. Lab. Ser., McGraw-Hill Book Co., Inc., New York, N. Y., vol. 15, p. 519, 1948.
[2] H. P. Westman, Ed., "Reference Data for Radio Engineers," ITT Handbook, Stratford Press, Inc., New York, N. Y. 4th ed., p. 556; 1957.
[3] *Ibid.*, p. 557.

* Received April 23, 1962. This work was performed at Sperry Gyroscope Co. under Contract AF 33(616)7278, sponsored by Electronic Components Lab., Aeronautical Systems Div., Wright Field, Dayton, Ohio.

[1] R. W. Gould and A. W. Trivelpiece, "A new mode of wave propagation on electron beams," *Proc. Symp. on Electronic Waveguides*, Polytechnic Press, Polytechnic Inst. of Brooklyn, Interscience Publishers, N. Y., vol. 8 pp. 215–228; April, 1958.
[2] L. D. Smullin and P. Chorney, "Propagation in ion loaded waveguides," *Proc. Symp. on Electronic Waveguides*, Polytechnic Press, Polytechnic Inst. of Brooklyn, Interscience Publishers, N. Y., vol. 8, pp 229–247; April, 1958.

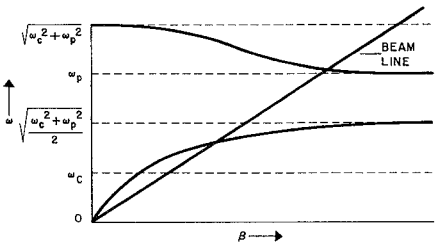

Fig. 3—ω-β curve for angularly symmetric mode.

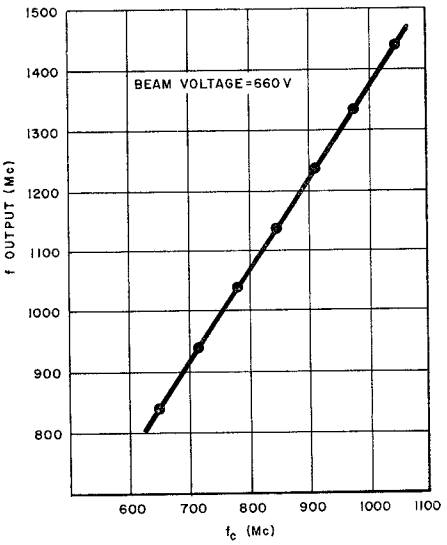

(a)

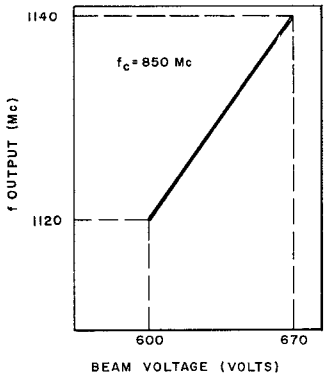

(b)

Fig. 4—Variations of output frequency.

formed analytically, using the determinantal equation given by Trivelpiece.[3])

At frequencies above ω_c, Trivelpiece[3] describes the mode as a surface wave, since charge builds up at the edge of the plasma and field discontinuities exist accordingly. In the surface wave region, the axial electric field is finite on the axis, and increases radially to the plasma edge. It then discontinuously falls to zero at the conducting wall. The coupling impedance on the axis of the plasma has been calculated to be slightly less than 1500 ohms for the actual operating parameters of this experiment.

[3] A. W. Trivelpiece, "Slow-Wave Propagation in Plasma Waveguides," C.I.T. Electron Tube and Microwave Lab., California Inst. of Technology, Pasadena, Calif., Tech. Rept. No. 7; 1958.

The oscillation mechanism can be explained in terms of reflections from objects situated along the plasma column. This is verified by the discreteness of the oscillation frequencies shown in Fig. 4(a). This graph shows that as the cyclotron frequency is varied, oscillations can only occur when the reflected wave adds constructively to the forward wave. Fig. 4(b) shows the variation of oscillation frequency with beam voltage when the cyclotron frequency is held constant. It is continuous because the range of oscillation frequencies is very small, and the entire line actually corresponds to a single point in Fig. 4(a). The increase of frequency for increasing voltage is seemingly incongruous with the voltage tuning characteristic of Fig. 3, but it should be remembered that ω_p varies with beam voltage for beam-generated plasma systems. Thus, for increased voltage, the upper cutoff frequency also increases, and the intersection of the beam line with the new ω-β curve will occur at a slightly higher frequency.

In summary, it is seen that an electron beam interacts very strongly with the surface wave mode of a plasma column; this interaction converts dc beam energy into narrow-band RF energy in the plasma.

P. J. Crepeau
Dept of Elec. Engrg.
Polytechnic Institute of Brooklyn
Brooklyn, N. Y.
T. Keegan
Republic Aviation Corp.
Farmingdale, N. Y.

A Double-Prism Attenuator for Millimeter Waves*

A double-prism attenuator, similar to the one built by Garnham[1] for use at 35 Gc, was built in the laboratory for use at 100 Gc and above. This attenuator utilizes the well-known fact that a wave which is incident on the interface between two dielectrics at an angle greater than the critical angle is totally reflected. If the wave is in a medium of index of refraction n and the other medium is free space the critical angle is

$$\theta_c = \sin^{-1}\frac{1}{n}.$$

* Received April 25, 1962. This research was supported by the Air Force Systems Command, United States Air Force.

[1] R. H. Garnham, "Optical and Quasi-Optical Transmission Techniques and Components Systems for Millimeter Wavelengths," Royal Radar Establishment, GT. Malvern, Eng., Rept. No. 3020; March, 1959.

If another medium of the same refractive index n is placed at a distance d from the first interface (Fig. 1), energy will be transferred into this new medium. The amount of coupled energy is a function of the distance d in terms of the wavelength.

For the case of a plane wave incident on the interface (the dielectric sheets extending to infinity), the amount of energy coupled to the new medium can be obtained analytically. Here we just state the results which are identical to Garnham's.

When the electric field is parallel to the plane of incidence

$$\left|\frac{E_t}{E_i}\right|^2 = \frac{4}{4\cosh^2 \alpha d + \dfrac{[(\epsilon+1)-(\epsilon^2+1)\sin^2\theta]^2 \sinh^2 \alpha d}{\epsilon(\epsilon\sin^2\theta - 1)\cos^2\theta}} \tag{1}$$

$$\left|\frac{E_r}{E_i}\right|^2 = \frac{(\epsilon-1)^2(\epsilon\sin^2\theta - \cos^2\theta)^2 \sinh^2 \alpha d}{4\epsilon\cos^2\theta(\epsilon\sin^2\theta - 1)\cosh^2 \alpha d + [(\epsilon+1)-(\epsilon^2+1)\sin^2\theta]^2 \sinh^2 \alpha d}, \tag{2}$$

where

$$\alpha = \frac{2\pi}{\lambda}(\epsilon\sin^2\theta - 1)^{1/2}.$$

There are corresponding equations for the case of perpendicular polarization.

A laboratory model of the double-prism attenuator was made of polystyrene. Each prism was half of a 2 inch cube (Fig. 2). The prism tolerance was ± 0.0015 inch.

The two prisms were mounted on a brass stand; one was movable and the other fixed. The base of the movable prism slid on two steel rods, its movement being controlled by a micrometer head. Fig. 3 shows the actual attenuator.

Although we realized that the matching of the outer surfaces was a factor necessary in obtaining good agreement between experimental and theoretical results, we neglected doing so because it would restrict the attenuator to a limited frequency range. If the surfaces are not perfectly flat and

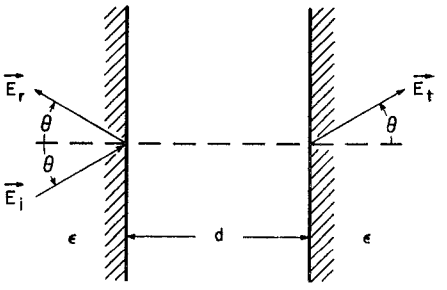

Fig. 1—Double interface arrangement.

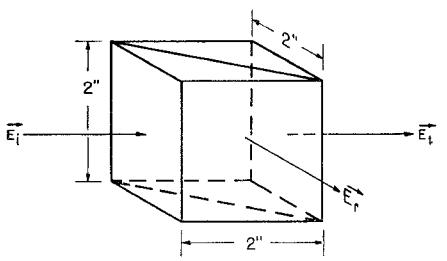

Fig. 2.—Double-prism attenuator.